Evaluation of the pore morphologies for piezoelectric energy harvesting application

Mingyang Yan [a], Shengwen Liu [a], Zhida Xiao [a], Xi Yuan [b], Di Zhai [a], Kechao Zhou [a], Dou Zhang[a], Guodong Zhang [a*], Chris Bowen [c], Yan Zhang [a*]

[a] State Key Laboratory of Powder Metallurgy, Central South University, Changsha, Hunan 410083, China.

[b] College of Chemistry and Chemical Engineering, Central South University, Changsha, Hunan 410083, China.

[c] Department of Mechanical Engineering, University of Bath, United Kingdom, Bath, BA27AY, UK

Corresponding Authors

[*] E-mail: 207024@csu.edu.cn (Guodong Zhang); yanzhangcsu@csu.edu.cn (Yan Zhang)

Abstract

Piezoelectric energy harvesting has attracted significant attention in recent years due to their high-power density and potential applications for self-powered sensor networks. In comparison to dense piezoelectric ceramics, porous piezoelectric ceramics exhibit superiority due to an enhancement of piezoelectric energy harvesting figure of merit. This paper provides a detailed examination of the effect of pore morphology on the piezoelectric energy harvesting performance of porous barium calcium zirconate titanate $0.5Ba(Zr_{0.2}\ Ti_{0.8})O_3$-$0.5(Ba_{0.7}Ca_{0.3})TiO_3$ (BCZT) ceramics. Three different pore morphologies of spherical, elliptical, and aligned lamellar pores were created via the burnt out polymer spheres method and freeze casting. The relative permittivity decreased with increasing porosity volume fraction for all porous BCZT ceramics. Both experimental and simulation results demonstrate that porous BCZT ceramics with aligned lamellar pores exhibit a higher remanent polarization. The longitudinal d_{33} piezoelectric charge coefficient decreased with increasing porosity volume fraction for the porous ceramics with three different pore morphologies; however, the rate of decrease in d_{33} with porosity is slower for aligned lamellar pores, leading to the highest piezoelectric energy harvesting figure of merit. Moreover, the peak power density of porous BCZT ceramics with aligned lamellar pores is shown to reach up to 38 $\mu W\ cm^{-2}$ when used as an energy harvester, which is significantly higher than that of porous BCZT ceramics with spherical or elliptical pores. This work is beneficial for the design and manufacture of porous ferroelectric materials in devices for piezoelectric energy harvesting applications.

Key words: porous BCZT ceramics, porosity, pore morphology, energy harvesting

1. Introduction

With the development of Internet of Things (IoT), there are increasing demands for sensors to detect a range of stimuli, including mechanical loads such as acceleration, force, pressure and strain. The growth in the number of sensors has also led to significant interest in energy harvesting technologies to reduce their reliance on batteries or wires to power such sensors.[1-3] Among the variety of energy harvesting technologies, piezoelectric energy harvesting, which converts ambient mechanical energy into electrical energy, has been considered to be a highly promising energy harvesting technology due to their high-power density and adaptability.[4-6]

Ferroelectric based ceramics are candidates for piezoelectric energy harvesting, primarily due to their high d_{ij} piezoelectric charge coefficients. The harvested energy density of a piezoelectric material subjected to a stress can be estimated by equation.[7]

$$FoM_{ij} = \frac{d_{ij}^2}{\varepsilon_0 \varepsilon_{33}^T} \quad (1)$$

where FoM_{ij} is a piezoelectric energy harvesting figure of merit under a mechanical stress, d_{ij} is the piezoelectric charge coefficient, ε_0 is the permittivity of free space, and ε_{33}^T is the relative permittivity at constant stress. It can be concluded from the above equation that piezoelectric materials with a high d_{ij} and low ε_{33}^T are highly desirable for energy harvesting applications.

In general, piezoelectric ceramics are produced to possess high relative densities

to achieve high piezoelectric properties.[8] However, the relative permittivity of dense ferroelectric ceramics is typically very high; for example, the relative permittivity of dense lead zirconate titanate (PZT) ceramic is ε_{33}^{T} ~ 1000 - 3000.[9] While the existence of porosity is often considered as defect, introducing porosity into a dense piezoelectric ceramics can act to reduce the relative permittivity,[10] which can therefore lead to an increase in FoM_{ij} and its performance for applications related to piezoelectric energy harvesting.[11] Thus, there is increasing interest in porous piezoelectric ceramics for energy harvesting applications. In the last few decades, a number of studies have been conducted to study the properties of porous piezoelectric ceramics, where a variety of studies have shown that the relative permittivity of porous piezoelectric ceramics decreased significantly with increasing porosity volume fraction due the introduction of low permittivity pores.[12-14] The piezoelectric charge coefficient d_{33} also decreased with increasing porosity volume fraction, but it decreased more slowly than that of the relative permittivity, leading to the improvement of piezoelectric energy harvesting figure of merit.[15-17] The pore shape can also have an influence on the properties of porous piezoelectric ceramics. Du et al. employed polymethyl methacrylate (PMMA) spheres and stearic acid (SA) to fabricate porous piezoelectric ceramics, and their results showed that the relative permittivity of porous ceramics formed using PMMA as pore-forming agent was higher than that using stearic acid, which was attributed to the pore shape and grain structure.[18] Yap et al. fabricated porous piezoelectric ceramics using polyethylene (PE) microspheres and fibers as pore-forming agents, and it was observed that porous piezoelectric ceramics with elliptical

pores possessed a lower remnant polarization, since the elliptical pores were perpendicular to the poling direction, leading to more regions of low electric field intensity during the polarization process.[19] An additional factor that influences the properties of porous piezoelectric ceramics is the pore orientation. ‘3-1’ type porous PZT ceramics with an aligned pore structure in the polarization direction were prepared via freeze casting by Guo et al., and a much higher permittivity was obtained compared to other types of porous PZT ceramics with the same porosity due to the highly aligned one-dimensional pore structure.[20] Zhang et al. fabricated a unidirectional porous ferroelectric ceramics via water-based freeze casting, and it was demonstrated that the relative permittivity, remnant polarization and hydrostatic figure of merits of a parallel-connected structure was higher than that of series-connected structure.[16] Subsequently, they compared the polarization-electric field (*P*-*E*) hysteresis loops of porous barium calcium zirconate titanate (BCZT) ceramics with randomly distributed pores and aligned pores.[21] It was observed that the remnant polarization of the ceramics with aligned pores decreased more slowly with an increase in pore volume fraction due to the existence of a higher fraction of poled regions in ceramics with aligned pores. Despite these developments, there continues to be challenges that need to be solved, where the effect of pore morphology of porous piezoelectric ceramics on the dielectric, piezoelectric properties and piezoelectric energy harvesting performance is still not clear.

In this paper, porous BCZT ceramics with three different pore morphologies of spherical, elliptical, and aligned lamellar pores were fabricated via burnt out polymer

spheres method and freeze casting. BCZT was selected due to its high piezoelectric charge coefficient of d_{33} ~ 620 pC N^{-1} and lead-free nature.[22] The effect of pore morphology on the dielectric, ferroelectric, piezoelectric properties and piezoelectric energy harvesting performance was systematically investigated. The results show that the peak power density of porous BCZT ceramics with aligned lamellar pores can reach up to 38 μW cm^{-2}, which is significantly higher than that of porous BCZT ceramics with spherical and elliptical pores. This work provides new insights in the understanding on the effect of pore morphology to inform future effort in the design of piezoelectric materials for piezoelectric energy harvesting applications.

2. Experimental procedure

Porous BCZT ceramics with three different pore morphologies were fabricated via burnt-out polymer spheres method and freeze casting. Firstly, BCZT powder was prepared by a solid-state reaction technique. Analytical grade $BaCO_3$ (99%), $CaCO_3$ (99%), TiO_2 (99%), and ZrO_2 (99%) were mixed and calcined at 1300 °C for 3 h and followed by additional ball-milling for 24 h. With regards to the burnt-out polymer spheres method, polymethyl methacrylate (PMMA) spheres with the diameter of 17 μm (Dongguan Kena Co. ltd., China) and carbon fibers with the diameter of 7 μm, length of 30 μm (Shenzhen, Tanxi Co. ltd., China) were selected as pore-forming agents. Fig. 1(a) shows the fabrication process of porous BCZT ceramics with spherical and elliptical pores. BCZT ceramic powders were mixed with PMMA spheres or carbon fibers, and the piezoelectric ceramic green bodies with an initial diameter of 12 mm and thickness of 1.0 mm were obtained via uniaxial hydraulic pressing with the pressure of

200 MPa. Then, the green bodies were sintered at 1350 °C for 3 h to obtain porous BCZT ceramics with spherical and elliptical pores. Porous BCZT ceramics with aligned lamellar pores were fabricated via freeze casting. As shown in Fig. 1(b), BCZT suspensions were ball-milled for 24 h to generate homogeneous suspensions, similar to our previous work.[16] The suspension was poured into a cylindrical polydimethylsiloxane (PDMS) mold (ϕ: 14 mm, H: 20 mm) and frozen in a liquid nitrogen container with a temperature gradient to form the aligned pore channels. Then, the samples were freeze-dried under vacuum condition to sublimate the ice crystals at -25°C and 1 Pa for 48 h. Finally, porous BCZT ceramics were sintered at 1350 °C for 3 h. Silver paste (Shenzhen Saiya Co. ltd., China) was painted on the upper and lower surfaces of the ceramics as electrodes, and porous BCZT ceramics with different pore morphologies were poled at 60 °C for 30 min using a DC voltage of 15 kV using a corona poling technique.

COMSOL Multiphysics 5.4 (combinations of Solid Mechanics, Electrostatics, and Electrical Circuit Modules) was used to simulate the electric field distribution of porous BCZT ceramics. Three models of porous BCZT ceramics with spherical, elliptical, and aligned lamellar pores were created, and the porosity of the three models was set to be 17 vol.%. Within the model the relative permittivity of unpoled BCZT was set to $\varepsilon_r \sim$ 2900, which was measured experimentally, and air with the relative permittivity of $\varepsilon_r =$ 1. An electric field of 2 kV/mm was applied to investigate the effect of pore morphology on the electric field distribution during the poling process.

The surface morphology of porous BCZT ceramics was observed by field emission

scanning electron microscopy (FESEM, NovaNanoSEM230, USA). The porosity level of porous BCZT ceramics was obtained by the Archimedes' method. The relative permittivity and dielectric loss were measured by Precision Impedance Analyzer (4294A; Agilent Technologies, Santa Clara, USA). The polarization-electric field (P-E) loops were characterized by a TF Analyzer 2000 (AixACCT systems, Germany). The piezoelectric charge coefficient was measured using a piezoelectric d_{33} meter (ZJ-4AN, Institute of Acoustics, Academic Sinica, China). The compressive strength of porous BCZT ceramics with different pore morphologies were tested with a crosshead speed of 0.5 mm/min by a universal mechanical testing machine (Instron 3369, USA). The piezoelectric energy harvesting performance of porous BCZT ceramics was evaluated via a programmable linear stepping motor, where a periodic compressive stress of 8 N at a specific frequency of 2 Hz was applied. The output voltage and current were measured by a digital multimeter with a resistance of 10 GΩ (Keithley DMM7510, Tektronix, USA). Porous BCZT ceramics were connected with different load resistances from 100 kΩ to 100 MΩ to obtain an optimized power density as a result of impedance matching. A capacitor of 1.0 μF was used to evaluate the charging performance of porous BCZT ceramics.

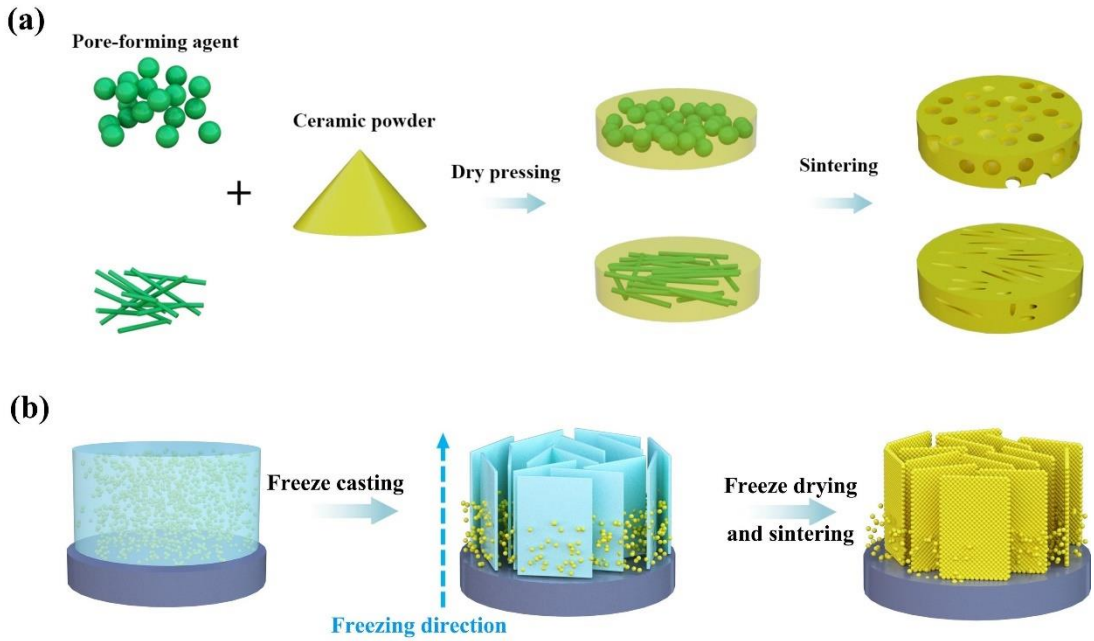

Fig. 1. Schematic for the fabrication process of porous BCZT ceramics. (a) burnt out polymer spheres method, (b) freeze casting.

3. Results and discussion

3.1 Microstructure

The microstructure of the porous BCZT ceramics with three different pore morphologies is shown in Fig. 2. As shown in Fig. 2(a)-(f), spherical pores were formed after the PMMA spheres were burnt out, since the pore shape is determined by the pore-forming agents. Isolated pores channels are observed when the porosity volume fraction is low, e.g.17 vol.%, but the pores begin to become interconnected at higher levels of porosity (37 vol.%). When the porosity is higher than 50 vol.%, the large numbers of pores became highly interconnected, as shown in Fig. 2(f). Porous BCZT ceramics created by the burnt-out polymer spheres method tend to transfer from a 3-0 structure at low porosity levels to a 3-3 structure at higher porosity levels due to the increasing

pore connectivity with increasing porosity, which is consistent with previous studies.[12, 23] Similar results are observed in porous BCZT ceramics fabricated by using carbon fibers as pore-forming agents. It can be seen from Fig. 2(g)-(l) that elliptical pores are randomly distributed in porous BCZT ceramics, and more pores are interconnected at higher porosity levels, which is a typical feature of porous piezoelectric ceramics created by the burnt-out polymer spheres method. Moreover, porous BCZT ceramics with aligned pore structure were manufactured via freeze casting. Aligned lamellar pore structure with ceramic bridges can be observed in all samples fabricated via freeze casting. When the porosity is lower than 20 vol.%, as shown in Fig. 2(m) and (n), the pore channels are increasingly indistinct as the porosity levels decrease, since the ceramic particles are not easily arranged to form aligned pores at higher ceramic loading levels.[24] The pore size increased as the porosity increased from 21 vol.% to 52 vol.%, and the pore channels became more distinct.

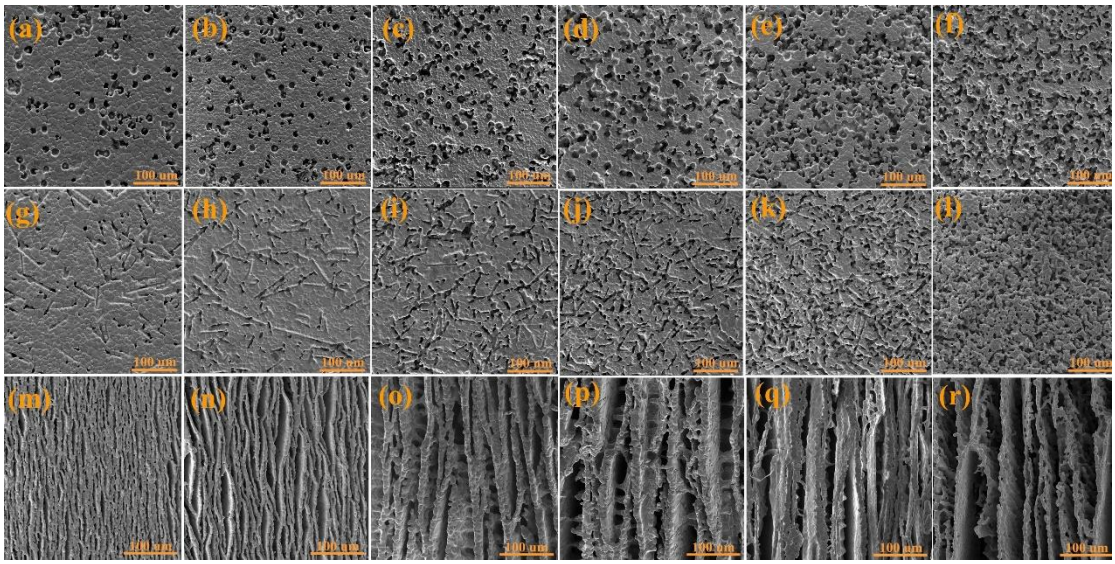

Fig. 2. SEM images of porous BCZT ceramics with spherical pores at different porosity levels. (a) 17 vol.%, (b) 27 vol.%, (c) 37 vol.%, (d) 43 vol.%, (e) 51 vol.%, (f) 55 vol.%;

SEM images of porous BCZT ceramics with elliptical pores at different porosity levels. (g) 17 vol.%, (h) 24 vol.%, (i) 30 vol.%, (j) 37 vol.%, (k) 43 vol.%, (l) 52 vol.%; SEM images of porous BCZT ceramics with aligned lamellar pores at different porosity levels. (m) 12 vol.%, (n) 21 vol.%, (o) 26 vol.%, (p) 31 vol.%, (q) 43 vol.%, (r) 52 vol.%.

3.2 Finite element modelling

Finite element modelling was used to demonstrate the effect of pore morphology on the electric field distribution of porous BCZT ceramics during the poling process. The modelling results are presented and summarized in Fig. 3 for an average electric field of 2 kV/mm applied from the top to the bottom of the material. With regards to dense BCZT ceramics, the electric field distribution is homogeneous and the applied electric field is higher than the coercive field. As a result, the dense BCZT ceramics can be completely poled. However, the introduction of pores into the dense BCZT ceramics can make the electric field distribution inhomogeneous, since most of the electric field concentrates in the low permittivity pore spaces. Regions of low electric field are mainly located in the ceramic in the immediate vicinity of the pore is the regions parallel to the direction of the applied electric field, while ceramic regions of high electric field are located near the pores in regions perpendicular to the direction of the applied field, which can be explained by an adaptation of Gauss' law.[9]

$$E_f = \frac{q}{A \cdot \varepsilon_0 \varepsilon_{33}^T}$$

where E_f is the local electric field, q is the charge, A is the electrode area, ε_0 is the permittivity of free space, and ε_{33}^T is the relative permittivity at constant stress.

Moreover, it can be observed that the applied electric field is concentrated in the low permittivity pore spaces for all porous BCZT ceramics of the three pore morphologies due to the relative permittivity mismatch between the ceramic phase and pores. A lower electric field is present in the higher permittivity piezoelectric ceramic phase. Although this general trend in the electric field distribution is similar, the magnitude of the electric field is different for three types of porous BCZT ceramics evaluated. In Fig. 3(a)-(c), the blue areas are those in which the electric field is relatively low and is lower than the coercive field (2 kV/mm), indicating that they are unpoled areas. As shown in Fig. 3d, the electric field is relatively homogenous with a strong peak slightly below E_{local} / $E_{applied}$ =1 in a dense BCZT ceramic (3 vol.% porosity). Porous BCZT ceramics with an aligned lamellar structure exhibit a lower peak electric field than dense ceramics, however, the peak electric field is much higher than the other two types of porous BCZT ceramics with spherical and elliptical pores, indicating that porous BCZT ceramics with aligned lamellar structure are more readily poled.

3.3 Dielectric properties

The dielectric properties of porous BCZT ceramics with different pore morphologies are now systematically investigated, including the relative permittivity and dielectric loss. Fig. 4 shows the relative permittivity of all porous BCZT ceramics with different porosity levels. For all the porous BCZT ceramics, the relative permittivity decreased with increasing frequency, since the ionic, space and spontaneous polarization cannot change in time with frequency, which is consistent with general ferroelectrics.[25, 26] As shown in Fig. 4(d), the relative permittivity of

all porous BCZT ceramics was lower than dense BCZT ceramic due to the introduction of low permittivity pores. Moreover, the relative permittivity of porous BCZT ceramics at 1 kHz decreased with an increase in porosity volume fraction, despite the difference in

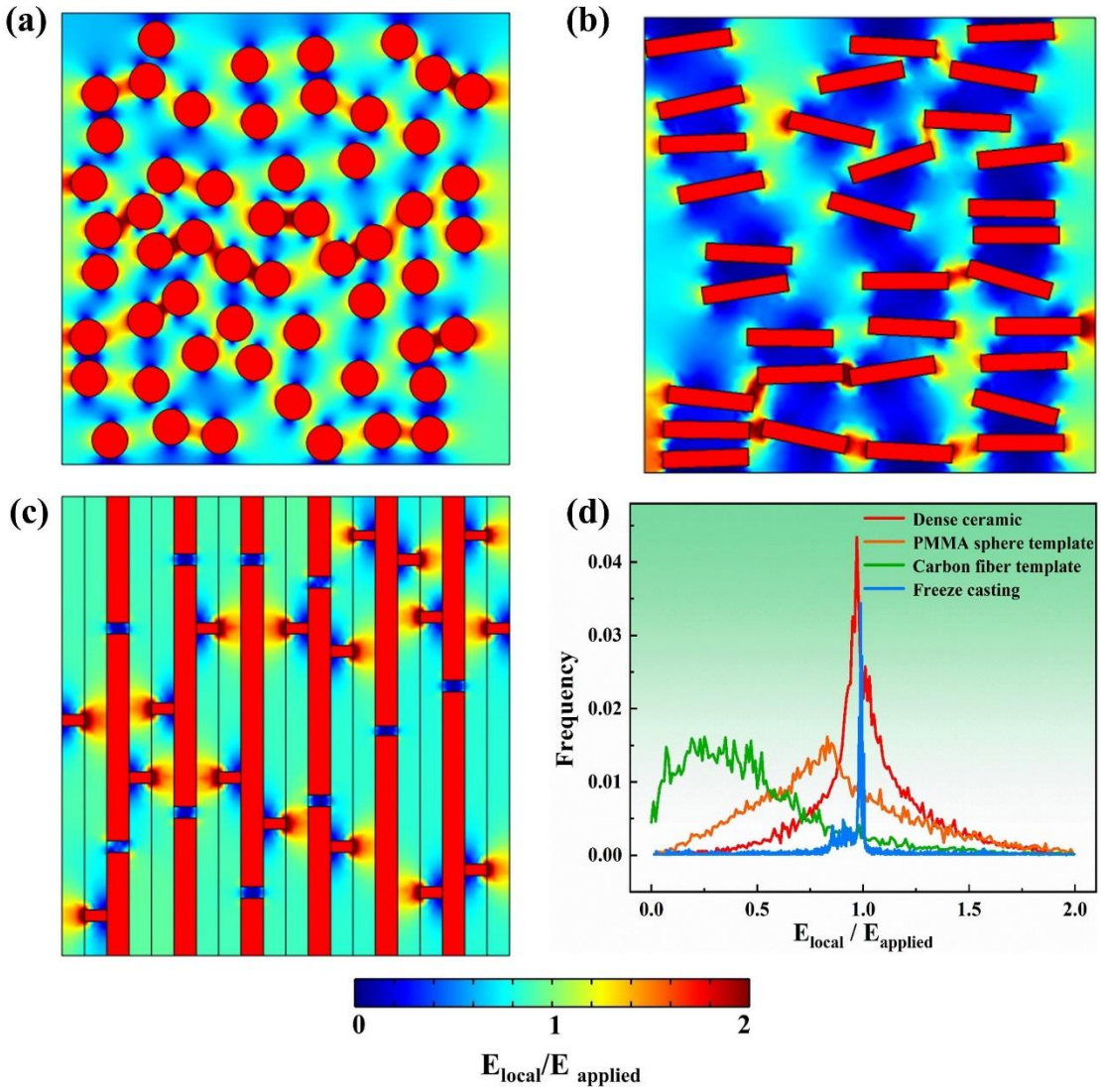

Fig. 3. Electric field distribution of porous BCZT ceramics (a) spherical pores, (b) elliptical pores, (c) aligned lamellar pores with ceramic bridges. (d) a comparison of the spectra for dense BCZT ceramic and porous BCZT ceramics with three different pore morphologies.

pore morphology, but the rate of decreasing in relative permittivity was different for the

different morphologies. For porous BCZT ceramics fabricated by the burnt-out polymer spheres method, the relative permittivity of samples with spherical pores is higher than those with elliptical pores. While porous BCZT ceramics with aligned lamellar pores have the highest relative permittivity compared with the other two types of porous

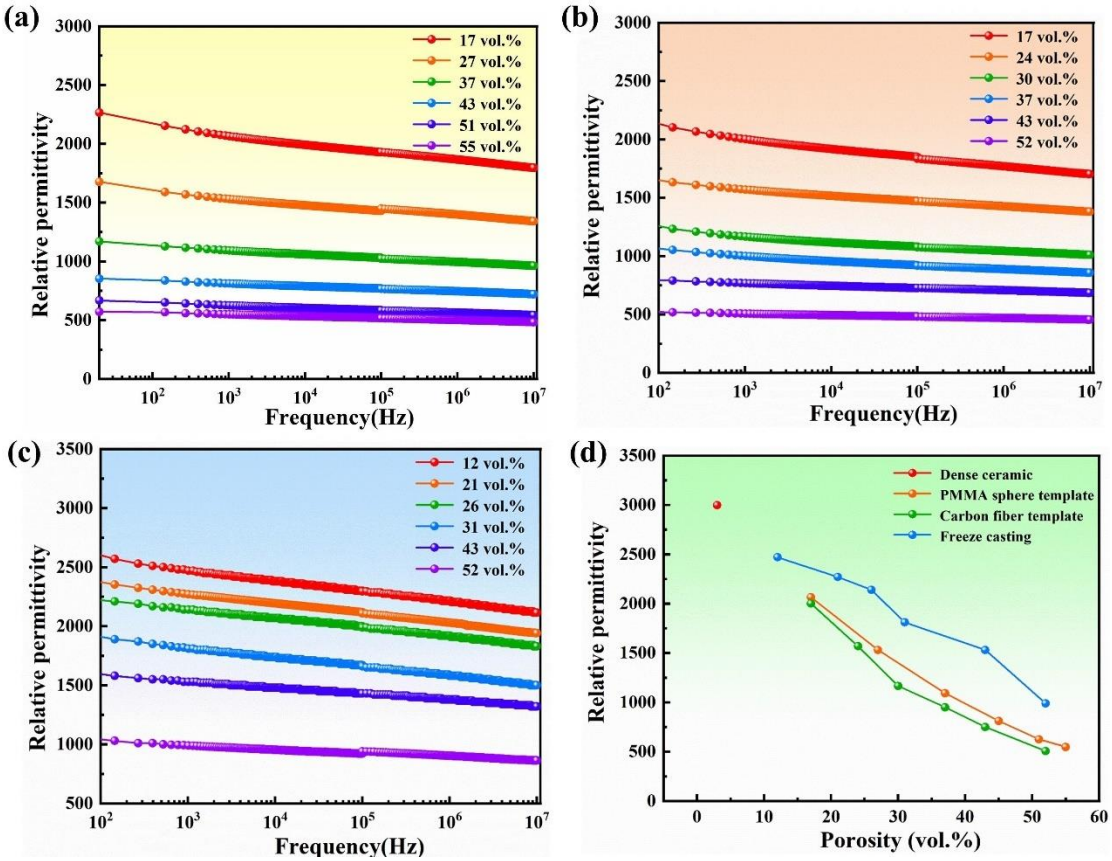

Fig. 4 The relative permittivity of unpoled porous BCZT ceramics. (a) spherical pores, (b) elliptical pores, (c) aligned lamellar pores. (d) a comparison of the relative permittivity for porous BCZT ceramics with three different pore morphologies.

BCZT ceramics. This different in relative permittivity can be ascribed to the pore shape. For porous BCZT ceramics fabricated by the burnt-out polymer spheres method, there exists a shape factor K_S (for spherical pores K_S = 1.0, for ellipsoidal pores, K_S = 0.5) according to previous theoretical models.[27-29] According to Banno's model,[18] the

relative permittivity is directly proportional to the shape factor K_S, and a higher shape factor will result in a higher relative permittivity. Therefore, porous BCZT ceramics with spherical pores have a higher relative permittivity than those with elliptical pores. However, the porous BCZT ceramics fabricated by freeze casting possessed the highest relative permittivity, which can be attributed to the greater connectivity of the high permittivity ceramic phase in the thickness direction. For the freeze-cast ceramics, the piezoelectric ceramic phase is highly aligned in the thickness direction, which leads to improved connectivity in the thickness direction than the other two types of porous BCZT ceramics with spherical and elliptical pores, leading to the highest relative permittivity.

The dielectric loss of porous BCZT ceramics with different morphologies is also evaluated. It can be seen from Fig. 5 that the dielectric loss initially decreased with increasing frequency due to a small level of DC conductivity in the ceramics and then began to increase at higher frequencies due to the ionic relaxation losses for all porous BCZT ceramics.[10, 30] The dielectric loss at 1 kHz of all porous BCZT ceramics with different porosities and pore morphologies remained at a low level of $tan\delta < 0.04$, which ensures the porous BCZT ceramics possess good dielectric properties for poling and use as a piezoelectric transducer for sensing or energy harvesting.

3.4 Ferroelectric properties

The polarization versus electric field (*P*-*E*) is an important tool to characterize porous piezoelectric ceramics, since it is directly related to the poling process. Fig. 6(a)-(c) shows the effect of porosity and pore morphologies on the *P*-*E* loops of porous

BCZT ceramics. The shape of hysteresis loops for all porous BCZT ceramics with different pore morphologies were symmetrical, demonstrating a good ferroelectric response and domain switching at all the samples investigated.[31] With increasing porosity levels, the remnant polarization (P_r) decreased for all porous BCZT ceramics due to the reduction of ceramic volume fraction, but the rate of decrease in P_r with increasing porosity level is different for the range of pore morphologies examined. The

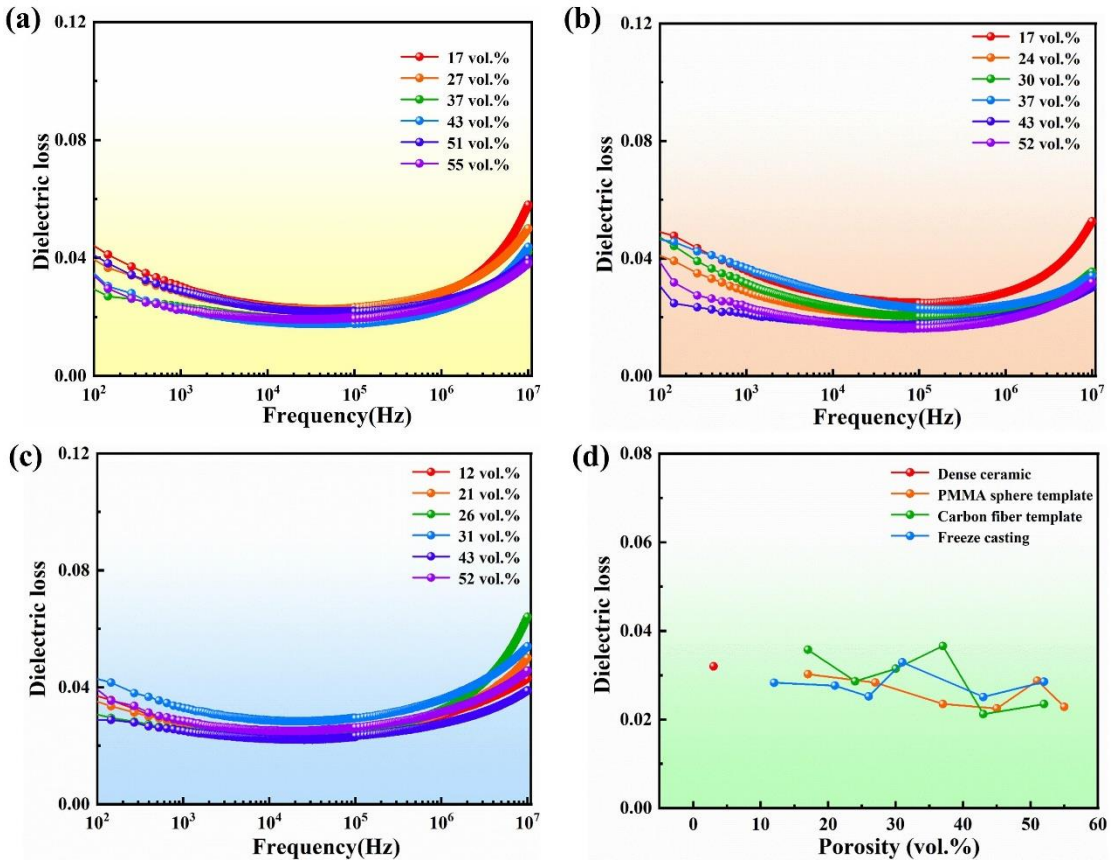

Fig. 5. The dielectric loss of unpoled porous BCZT ceramics. (a) spherical pores, (b) elliptical pores, (c) aligned lamellar pores. (d) a comparison of the dielectric loss for porous BCZT ceramics with three different pore morphologies.

P_r of porous BCZT ceramics with aligned pores decreased from 6.8 μC cm^{-2} to 3.2 μC cm^{-2}, while for porous BCZT ceramics with elliptical pores, the P_r decreased more rapidly with increasing porosity from 5.6 μC cm^{-2} to 1.1 μC cm^{-2}. The difference in

remnant polarization is due to the pore morphology, where it is demonstrated from the simulation results that porous BCZT ceramics with aligned pores are more readily poled compared with the other two types of porous BCZT ceramics due to the higher electric field distribution, see Fig. 3(d), leading to higher remnant polarization. Porous BCZT ceramics with elliptical pores have the least poled regions and the lowest electric field in Fig. 3(d), therefore, the remnant polarization is the lowest.

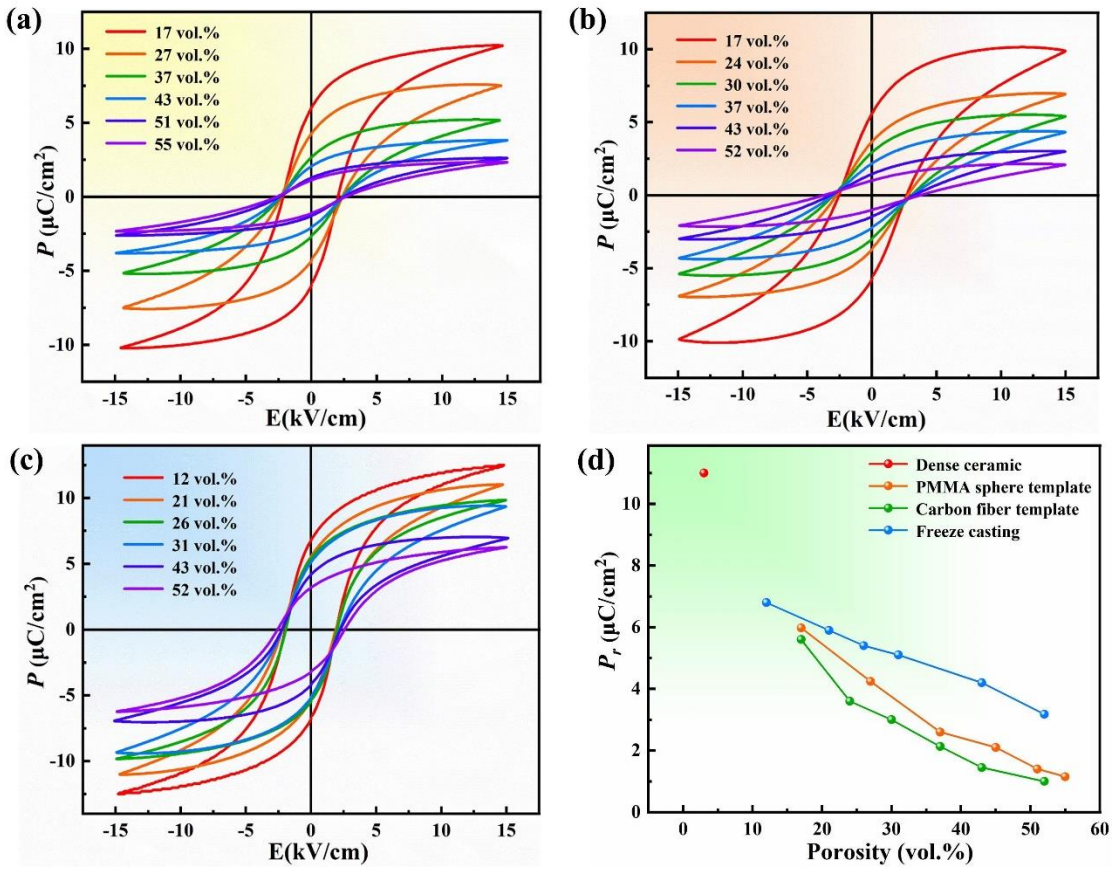

Fig. 6. P-E loops of porous BCZT ceramics (a) spherical pores, (b) elliptical pores, (c) aligned lamellar pores. (d) a comparison of remnant polarization for porous BCZT ceramics with three different pore morphologies.

The effect of pore morphology on the coercive field (E_c) was also studied. As shown in Fig. 7, the E_c of porous BCZT ceramics with spherical and elliptical pores increased with increasing porosity volume fraction. However, the E_c of porous BCZT

ceramics with aligned lamellar pores decreased with an increase in porosity volume fraction when the porosity was lower than 23 vol.%, then began to increase with a further increase in porosity levels, which is consistent with our previous report.[21] There is a turning point in the dependence of E_c with a corresponding porosity range of 20 - 25 vol.% and is a result of the more complex electric field distribution in the more porous ceramics. Moreover, it can be observed that porous BCZT ceramics with elliptical pores have the highest coercive field, indicating that they are more difficult to be fully poled; again, this is due to the lower overall electric field in this type of microstructure, as seen in Figure 3(d). The coercive field of porous BCZT ceramics with aligned lamellar pores is the lowest for all porosity levels, therefore, porous BCZT ceramics with aligned lamellar pores are more easily to be poled and have the highest remnant polarization.

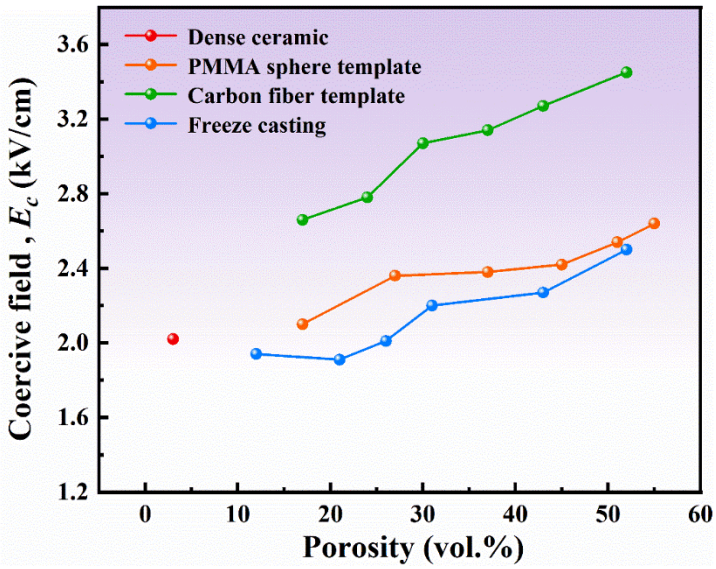

Fig. 7. Coercive field (E_c) of porous BCZT ceramics with porosity for different pore morphologies

3.5 Piezoelectric properties and energy harvesting performance

The piezoelectric properties and energy harvesting performance are also investigated. Fig. 8(a) shows the variation of the longitudinal d_{33} piezoelectric charge coefficient of porous BCZT ceramics with three pore morphologies at different porosity levels. It can be observed that the d_{33} piezoelectric coefficient decreased with increasing porosity volume fraction, but again the rate of decrease varies with pore morphology. The d_{33} piezoelectric coefficient decreased from 500 pC/N to 355 pC/N for porous BCZT ceramics with aligned lamellar pores, which decreased more slowly with increasing porosity level than materials with randomly distributed spherical or elliptical pores. Porous BCZT ceramics with elliptical pores possessed the lowest d_{33} piezoelectric coefficient, which can be attributed to less poled regions in BCZT ceramics; see Figure 3d. The effect of pore morphology on the piezoelectric energy harvesting figure of merit (FoM_{33}) is presented in Fig. 8(b). It can be observed that the piezoelectric energy harvesting figure of merit increase with an increase in porosity levels. Porous BCZT ceramics with aligned pore structure have the highest FoM_{33} due to the high d_{33} piezoelectric coefficient, which exhibit potential for the applications of piezoelectric energy harvesting and sensing.

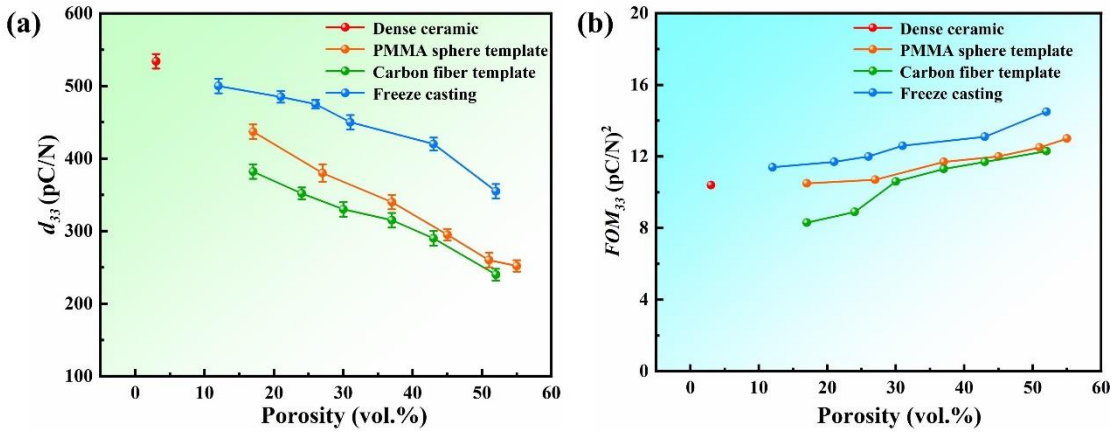

Fig. 8. Comparison of piezoelectric properties for porous BCZT ceramics. (a)

piezoelectric coefficient (d_{33}), (b) piezoelectric energy harvesting figure of merit (FOM_{33}).

To evaluate the piezoelectric energy harvesting performance, the mechanical properties of dense and porous BCZT ceramics with the porosity of 30 vol.% are investigated, since they need to operate in a vibrating environment for a long period. As shown in Fig. 9, dense BCZT ceramics exhibit the highest compressive strength of 63.5 MPa. However, for porous BCZT ceramics with different pore morphologies, the porous BCZT ceramics with aligned lamellar pore structure possess the higher compressive strength than the ceramics with a randomly distributed pore structure, which is in accordance with the results of previous reports.[11, 32] The main reason of the higher strength can be attributed to the aligned pore structure, since the ceramics particles are aligned in the direction of loading and help to carry and transfer the load through the porous structure. Therefore, porous BCZT ceramics with aligned pore structure are more suitable for piezoelectric energy harvesting applications, when they work in a vibrating environment for a long period.

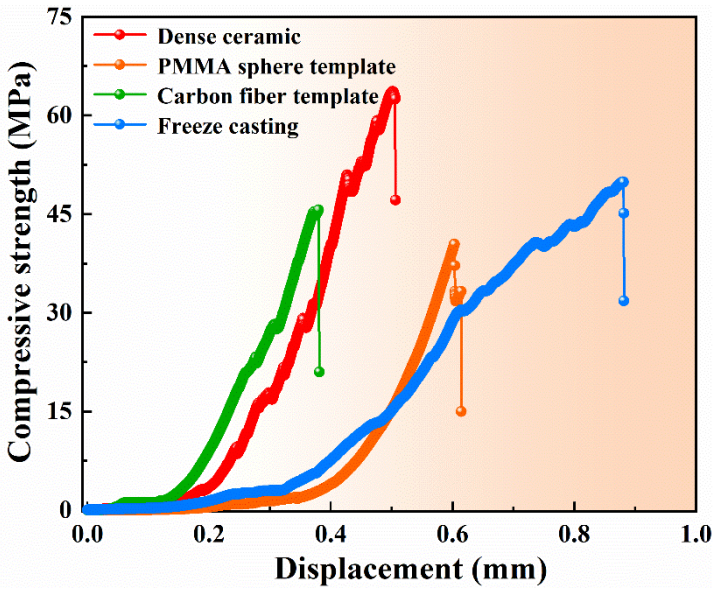

Fig. 9. Compressive strength of dense and porous BCZT ceramics with different pore morphologies.

The piezoelectric energy harvesting performance of porous BCZT ceramics with a porosity of 30 vol.% is now evaluated, including output voltage, current and power density. The area of dense and porous BCZT ceramics is 88 ± 0.5 mm^2, and the thickness is 0.9 ± 0.05 mm. A schematic of the piezoelectric energy harvesting device is presented in Fig. 10(a), which provides a periodic compressive stress of 8 N at a frequency of 2 Hz during the testing process. Fig. 10(b) shows the output voltage of dense BCZT ceramic and porous BCZT ceramics with three different pore morphologies. It can be observed that porous BCZT ceramic with spherical pores had the highest open circuit output voltage, which can be attributed to the high piezoelectric voltage coefficient of this material. The open circuit voltage generated by a piezoelectric ceramic can be described by the following equation:[33]

$$V_{oc} = \frac{d_{33}}{\varepsilon_0 \varepsilon_{33}^{\mathrm{T}}} \cdot t \cdot \sigma = g_{33} \cdot t \cdot \sigma \quad (2)$$

where V_{oc} is the open circuit voltage of piezoelectric materials, d_{33} is the piezoelectric charge coefficient, ε_{33}^{T} is the relative permittivity, t is the thickness of piezoelectric ceramics, and σ is the applied stress. Therefore, porous BCZT ceramics with a higher piezoelectric voltage coefficient (g_{33}) can generate a higher output voltage. The short circuit output current of porous BCZT ceramics is presented in Fig. 10(c). The highest output current was obtained in dense BCZT ceramic, while the porous BCZT ceramics with aligned lamellar pores possessed higher output current than those with spherical and ellipticals pores. The output current generated by the piezoelectric

ceramics can be evaluated by the following equation:

$$I_{sc} = \frac{dQ}{dt} = d_{33}\frac{dF}{dt} = d_{33}\mathrm{A}\frac{d\sigma}{dt} \quad (3)$$

where I_{sc} is the short circuit current, d_{33} is the piezoelectric charge coefficient, Q is the charge (where $Q = d_{33}.F$), F is the applied force, and A is the electrode area. It can be concluded from the equation that the output current is proportional to the d_{33} piezoelectric coefficient and the rate of change of force. Thus, porous BCZT ceramics with aligned lamellar pores had a higher short circuit current compared with the other two types of porous BCZT ceramics due to the higher d_{33} coefficient; see Fig. 8(a). Porous BCZT ceramics were employed to charge the capacitor of 1.0 μF to evaluate the capability of charge, and the relevant circuit diagram for charging the capacitor is presented in Fig. 10(d). As shown in Fig. 10(e), the measured voltage increases rapidly at the start of charging process and gradually reaches a saturation voltage.[34, 35] The saturation value is different for porous BCZT ceramics with three pore morphologies, which is consistent with the change of piezoelectric voltage coefficient.

Fig. 10(f) shows the output power density of porous BCZT ceramics as a function of load resistance ranging from 100 kΩ to 100 MΩ. For dense and porous BCZT ceramics, the output power density initially increased with an increase of load resistance, and then decreased at higher load resistances. Porous BCZT ceramic with the aligned pore structure possessed the highest power density of 38 μWcm^{-2} with an optimal load resistance of 1.5 MΩ, which is two times higher than that of the dense BCZT ceramic. The reason can be attributed to the excellent piezoelectric properties and energy

harvesting figure of merit induced by the aligned porosity; since the harvesting figure of merit is proportional to $\frac{d_{ij}^2}{\varepsilon_{33}^T}$, the high d_{33} coefficients are beneficial for harvesting.

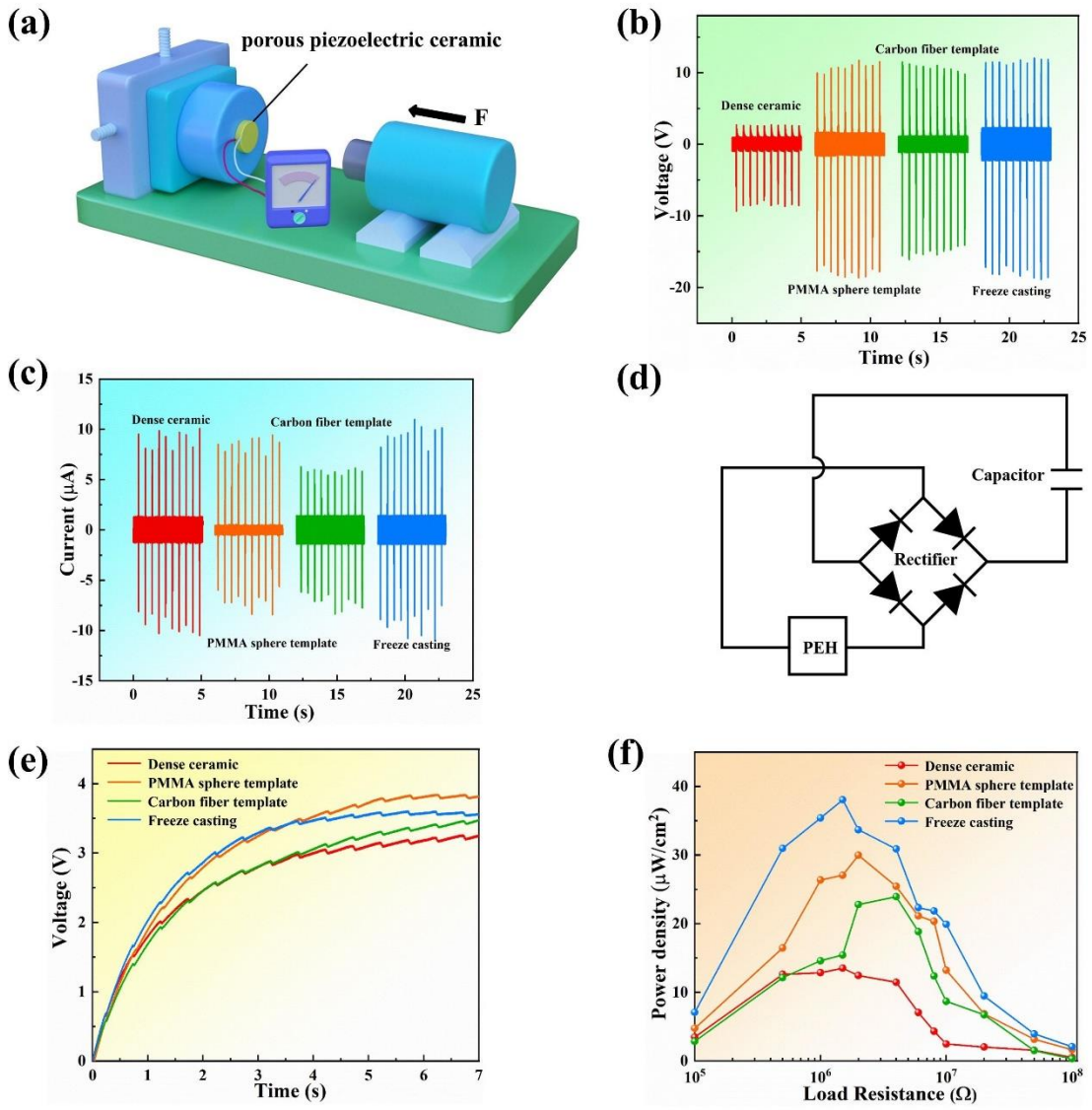

Fig. 10. Comparison of piezoelectric energy harvesting performance for porous BCZT ceramics. (a) schematic of the measurement of piezoelectric energy harvesting performance, (b) output voltage, (c) output current, (d) circuit diagram for charging the capacitor, (e) time dependent charging curves, (f) output power density.

4. Conclusion

This paper has demonstrated the effect of pore morphology on the dielectric, ferroelectric, piezoelectric properties, and energy harvesting performance of porous BCZT ceramics. Porous BCZT ceramics with spherical, elliptical, and aligned lamellar pore structures were fabricated by burnt out polymer spheres method and freeze casting. The relative permittivity decreased with increasing porosity, however the rate of decreasing in permittivity with porosity level varied with pore morphology; porous BCZT ceramics with aligned pore structure had the highest relative permittivity. Finite element modelling show that porous BCZT ceramics with an aligned pore structure are more easily poled compared with materials with spherical or elliptical pores due the presence of a narrower and higher electric field distribution within the microstructure. Moreover, porous BCZT ceramics with aligned lamellar pores exhibit a higher remanent polarization due to the higher electric field distribution. Compared with the porous BCZT ceramics with spherical or elliptical pores, the d_{33} piezoelectric coefficient decreased more slowly with increasing pore fraction, leading to higher piezoelectric energy harvesting figure of merit. The piezoelectric energy harvesting performance was also evaluated, porous BCZT ceramics with aligned lamellar pores possessed the highest peak power density of 38 $\mu W\ cm^{-2}$, which is significantly higher than that of porous BCZT ceramics with spherical and elliptical pores. In addition, porous BCZT ceramics are demonstrated to have the ability to successfully charge capacitors. This work therefore provides a deeper understanding on the effect of pore

morphology and expands the applications of porous piezoelectric ceramics for piezoelectric energy harvesting.

Acknowledgements

The authors acknowledge the National Natural Science Foundation of China (No. U19A2087), Key Research and Development Project of Hunan Province (No. 2020WK2004), Overseas Talent Introduction Project of China, Hundred Youth Talents Program of Hunan and State Key Laboratory of Powder Metallurgy, Central South University, Changsha, China, The Leverhulme Trust (RGP-2018-290).

Declaration of Competing Interest

The authors declare that they have no known competing financial interests or personal relationships that could have appeared to influence the work reported in this paper.

References

[1] Y. Zhang, P.T.T. Phuong, E. Roake, H. Khanbareh, Y. Wang, S. Dunn, C. Bowen, Thermal Energy Harvesting Using Pyroelectric-Electrochemical Coupling in Ferroelectric Materials, Joule, 4 (2020) 301-309.

[2] H. Li, C.R. Bowen, Y. Yang, Scavenging Energy Sources Using Ferroelectric Materials, Adv. Funct. Mater., 31 (2021) 2100905.

[3] T. Zhang, Z. Wen, Y. Liu, Z. Zhang, Y. Xie, X. Sun, Hybridized Nanogenerators for Multifunctional Self-Powered Sensing: Principles, Prototypes, and Perspectives, iScience, 23 (2020) 101813.

[4] C.R. Bowen, H.A. Kim, P.M. Weaver, S. Dunn, Piezoelectric and ferroelectric materials and structures for energy harvesting applications, Energy Environ. Sci., 7 (2014) 25-44.

[5] N. Sezer, M. Koç, A comprehensive review on the state-of-the-art of piezoelectric energy harvesting, Nano Energy, 80 (2021) 105567.

[6] F. Ali, W. Raza, X. Li, H. Gul, K.-H. Kim, Piezoelectric energy harvesters for biomedical applications, Nano Energy, 57 (2019) 879-902.

[7] Y. Zhang, M. Xie, J. Roscow, Y. Bao, K. Zhou, D. Zhang, C.R. Bowen, Enhanced pyroelectric and piezoelectric properties of PZT with aligned porosity for energy harvesting applications, J. Mater. Chem. A, 5 (2017) 6569-6580.

[8] J. Hao, W. Li, J. Zhai, H. Chen, Progress in high-strain perovskite piezoelectric ceramics, Mater. Sci. Eng. R Rep., 135 (2019) 1-57.

[9] J.I. Roscow, R.W.C. Lewis, J. Taylor, C.R. Bowen, Modelling and fabrication of

porous sandwich layer barium titanate with improved piezoelectric energy harvesting figures of merit, Acta Mater., 128 (2017) 207-217.

[10] Y. Zhang, M. Xie, J. Roscow, C. Bowen, Dielectric and piezoelectric properties of porous lead-free $0.5Ba(Ca_{0.8}Zr_{0.2})O_3$-$0.5(Ba_{0.7}Ca_{0.3})TiO_3$ ceramics, Mater. Res. Bull., 112 (2019) 426-431.

[11] Y. Zhang, Y. Bao, D. Zhang, C.R. Bowen, L. Pilon, Porous PZT Ceramics with Aligned Pore Channels for Energy Harvesting Applications, J. Am. Ceram. Soc., 98 (2015) 2980-2983.

[12] H. Zhang, J. Li, B. Zhang, Microstructure and electrical properties of porous PZT ceramics derived from different pore-forming agents, Acta Mater., 55 (2007) 171-181.

[13] T. Zeng, X. Dong, C. Mao, Z. Zhou, H. Yang, Effects of pore shape and porosity on the properties of porous PZT 95/5 ceramics, J. Eur. Ceram. Soc., 27 (2007) 2025-2029.

[14] Q. Wang, Q. Chen, J. Zhu, C. Huang, B.W. Darvell, Z. Chen, Effects of pore shape and porosity on the properties of porous LNKN ceramics as bone substitute, Mater. Chem. Phys., 109 (2008) 488-491.

[15] D.J. Shin, D.H. Lim, B.K. Koo, M.S. Kim, I.S. Kim, S.J. Jeong, Porous sandwich structures based on $BaZrTiO_3$–$BaCaTiO_3$ ceramics for piezoelectric energy harvesting, J. Alloy. Compd., 831 (2020) 154792.

[16] Y. Zhang, J. Roscow, M. Xie, C. Bowen, High piezoelectric sensitivity and hydrostatic figures of merit in unidirectional porous ferroelectric ceramics

fabricated by freeze casting, J. Eur. Ceram. Soc., 38 (2018) 4203-4211.

[17] J.I. Roscow, Y. Zhang, M.J. Kraśny, R.W.C. Lewis, J. Taylor, C.R. Bowen, Freeze cast porous barium titanate for enhanced piezoelectric energy harvesting, J. Phys. D-Appl. Phys., 51 (2018) 225301.

[18] L. Du, X. Du, L. Zhang, Q. An, W. Ma, H. Ran, H. Du, Effect of closed pores on dielectric properties of $0.8Na_{0.5}Bi_{0.5}TiO_3$-$0.2K_{0.5}Bi_{0.5}TiO_3$ porous ceramics, J. Eur. Ceram. Soc., 38 (2018) 2767-2773.

[19] E.W. Yap, J. Glaum, J. Oddershede, J.E. Daniels, Effect of porosity on the ferroelectric and piezoelectric properties of $(Ba_{0.85}Ca_{0.15})(Zr_{0.1}Ti_{0.9})O_3$ piezoelectric ceramics, Scr. Mater., 145 (2018) 122-125.

[20] R. Guo, C.A. Wang, A. Yang, Effects of pore size and orientation on dielectric and piezoelectric properties of 1–3 type porous PZT ceramics, J. Eur. Ceram. Soc., 31 (2011) 605-609.

[21] Y. Zhang, J. Roscow, R. Lewis, H. Khanbareh, V.Y. Topolov, M. Xie, C.R. Bowen, Understanding the effect of porosity on the polarisation-field response of ferroelectric materials, Acta Mater., 154 (2018) 100-112.

[22] W. Liu, X. Ren, Large piezoelectric effect in Pb-free ceramics, Phys Rev Lett, 103 (2009) 257602.

[23] J. Tan, Z. Li, Fabrication and electrical properties of porous BS–0.64PT high temperature piezoceramics using polystyrene microsphere, Ceram. Int., 41 (2015) S414-S420.

[24] Y. Zhang, L. Chen, J. Zeng, K. Zhou, D. Zhang, Aligned porous barium

titanate/hydroxyapatite composites with high piezoelectric coefficients for bone tissue engineering, Mater Sci Eng C Mater Biol Appl, 39 (2014) 143-149.

[25] W. Wang, M. Zhang, L. Xin, S. Shen, J. Zhai, Effect of interface behavior on dielectric properties of ferroelectric-dielectric composite ceramics, J. Alloy. Compd., 809 (2019) 151712.

[26] H. Nie, X. Dong, N. Feng, X. Chen, G. Wang, Y. Gu, H. He, Y. Liu, Microgeometry effect on the properties of $Pb_{0.99}(Zr_{0.95}Ti_{0.05})_{0.98}Nb_{0.02}O_3$ ferroelectric ceramics, Mater. Res. Bull., 46 (2011) 1243-1246.

[27] A. Yang, C.A. Wang, R. Guo, Y. Huang, Microstructure and Electrical Properties of Porous PZT Ceramics Fabricated by Different Methods, J. Am. Ceram. Soc., 93 (2010) 1984.

[28] P.W. Bosse, K.S. Challagulla, T.A. Venkatesh, Effects of foam shape and porosity aspect ratio on the electromechanical properties of 3-3 piezoelectric foams, Acta Mater., 60 (2012) 6464-6475.

[29] T. Zeng, X. Dong, C. Mao, S. Chen, H. Chen, Preparation and properties of porous PMN–PZT ceramics doped with strontium, Mater. Sci. Eng. B, 135 (2006) 50-54.

[30] M. Chen, Y. Pu, L. Zhang, Phase transition behavior, dielectric and ferroelectric properties of $(1-x)NaNbO_3$-$xLiTaO_3$ ceramics, J. Alloy. Compd., 877 (2021) 160225.

[31] S. Zhu, L. Cao, Z. Xiong, C. Lu, Z. Gao, Enhanced piezoelectric properties of 3-1 type porous $0.94Bi_{0.5}Na_{0.5}TiO_3$-$0.06BaTiO_3$ ferroelectric ceramics, J. Eur. Ceram. Soc., 38 (2018) 2251-2255.

[32] A. Lichtner, D. Roussel, D. Jauffrès, C.L. Martin, R.K. Bordia, G. Franks, Effect of Macropore Anisotropy on the Mechanical Response of Hierarchically Porous Ceramics, J. Am. Ceram. Soc., 99 (2015) 979-987.

[33] R.A. Surmenev, R.V. Chernozem, I.O. Pariy, M.A. Surmeneva, A review on piezo- and pyroelectric responses of flexible nano- and micropatterned polymer surfaces for biomedical sensing and energy harvesting applications, Nano Energy, 79 (2021) 105442.

[34] Y. Sun, J. Chen, X. Li, Y. Lu, S. Zhang, Z. Cheng, Flexible piezoelectric energy harvester/sensor with high voltage output over wide temperature range, Nano Energy, 61 (2019) 337-345.

[35] S.K. Ghosh, D. Mandal, Synergistically enhanced piezoelectric output in highly aligned 1D polymer nanofibers integrated all-fiber nanogenerator for wearable nano-tactile sensor, Nano Energy, 53 (2018) 245-257.